CALCULATION OF HEAD RELATED TRANSFER FUNCTIONS IN THE PROXIMITY REGION USING SPHERICAL HARMONICS DECOMPOSITION: COMPARISON WITH MEASUREMENTS AND EVALUATION

Khoa-Van Nguyen, Thibaut Carpentier, Markus Noisternig, Olivier Warusfel

IRCAM – CNRS UMR STMS
1 place Igor-Stravinksy, 75004, Paris, France
{khoa-van.nguyen, thibaut.carpentier}@ircam.fr
{markus.noisternig, olivier.warusfel}@ircam.fr

ABSTRACT

This article describes a comparison between different compensation and range extrapolation methods to predict head related transfer functions (HRTFs) in the proximity of the head, and acoustic measurements of a *HEAD acoustics* dummy head in an anechoic room. An extensive set of left and right ear impulse responses was measured on a dense angular grid over an open sphere at eight different distances from the head, providing a total of 6920 measurement positions. In this study, HRTF data is represented in the spherical wave spectrum, turning the range extrapolation problem into an acoustic radiation problem. The radial extrapolation is calculated from a given set of HRTFs at a fixed distance, from near-field to far-field and vice versa. The prediction based on spherical harmonics is compared with methods such as the inverse distance attenuation coefficient, a near-field compensation filter, and a geometrical approach for the selection of HRTFs. A spectral distortion measure is computed to quantify the similarity between predicted HRTFs and actual measurements. The data fit between predicted and measured HRTFs is correct for most of the different methods but the spherical harmonics method provides more convincing results especially for near-field prediction at low and medium frequencies.

1. INTRODUCTION

Binaural rendering is a three dimensional sound spatialization technique for headphone listening that has been widely used for Virtual Auditory Displays (VAD) and that becomes more and more integrated into Virtual Reality (VR) environments. Its principle is based on applying position dependent spatial filters, the head related transfer functions (HRTF), to a monophonic sound signal. The HRTFs cumulate all scattering effects of the ears, the head and torso and, as a consequence, are able to create the illusion of a spatially located sound.

HRTFs are typically measured for a large number of positions on a surrounding sphere in the far-field of the head. This finite set of HRTFs is used to synthesize any other angular and/or radial source position by applying different interpolation or range extrapolation methods.

Angular interpolation methods can be categorized into two main categories: local interpolation techniques using neighboring HRTFs [1, 2], and global interpolation techniques based on the analysis and decomposition of the complete set of measured HRTFs, for instance the principal component analysis (PCA) [3, 4] or the spherical harmonics decomposition [5].

The range extrapolation of HRTFs, especially towards the near-field, has drawn the attention of researchers since Brungart and Rabinowitz [6] discussed the physical and perceptual differences of near-field and far-field HRTFs. They have shown that far-field HRTFs cannot be used to synthesize virtual sound sources in the near-field.

The perceived distance of a sound source in a room mainly depends on the direct-sound-to-reverb ratio, and the distance-dependent level attenuation and high-frequency damping. These effects are commonly applied to create a distance effect in virtual audio environments [7]. It is obvious that these algorithms cannot be applied to sources in the near-field of the listener. Romblom and Cook [8] therefore proposed an efficient method based on near-field compensation filters and a geometric approach for the selection of HRTFs. Lentz et al. [9] perceptually evaluated sets of HRTFs measured at different distances from the head. The results show limits of noticeable differences between near-field and far-field HRTFs.

Interpolation and range extrapolation of HRTFs can be reformulated as acoustic radiation and scattering problem, which is commonly expanded into spherical base functions, cf. [10, 11]. The angular interpolation using spherical harmonics was first presented in [5] using a Gaussian quadrature method to determine the measurement points on the sphere. This method was further extended to irregular and open sampling grids applying appropriate regularization methods [12]. Comparisons between measured and reconstructed HRTFs have shown accurate simulation results. Range extrapolation of HRTFs applying spherical Hankel functions, as radial solutions of the wave equation, was proposed in [13] and [14]. This method was numerically simulated and further evaluated on a spherical head model [15]. However, to the best knowledge of the authors, it was never compared against measurement results.

This article presents a comparison of the spherical acoustics expansion method for the prediction of near-field HRTFs and measurements of a *HEAD acoustics* mannequin in an anechoic room. The radial extrapolation is calculated from a given set of HRTFs at a fixed distance, from near-field to far-field and vice versa. The prediction based on spherical harmonics is compared to other simulation methods, such as the inverse distance attenuation coefficient, near-field compensation filters, and geometrical approaches for the selection of HRTFs. Practical issues such as a low signal-to-noise ratio (SNR), or well distributed spherical

†This research was supported in part by French ANR RIAM 004 02 “EarToy”.

sampling points are further discussed as they may considerably prevent an accurate reconstruction of HRTFs, especially for the near-field prediction method [10].

2. REVERSE HRTF MEASUREMENTS AT DIFFERENT DISTANCES

2.1. Apparatus

All HRTF data was measured in an anechoic room (5.9 × 4.4 × 4.25 m^3) at IRCAM with a low cut-off frequency of 75 Hz. The measurement system consists of a *Bruel & Kjaer* turntable and a custom-build Midi controlled rotating arm that can be equipped with loudspeakers and/or microphones. The center point of the measurement system is determined by the intersection of three laser beams: one that is vertically aligned with the rotation axis of the turntable, and two that are horizontally aligned with the rotation axis of the mechanical arm, hence defining the interaural axis.

For this study, a *HEAD acoustics* dummy head was mounted on the turntable and aligned with the main axis of rotation. The reciprocity measurement method [16] was applied for acoustic measurements, assuming that the microphone and loudspeaker positions can be reversed. A *Knowles ED29689* loudspeaker was positioned at the entrance of the dummy head's ear canal and the emitted sound was captured by an array of microphones. This array consists of eight *Monaccor MCE 2000* omnidirectional microphones mounted on a 170 cm rod perpendicular to the mechanical arm, pointing towards the center of the measurement system, which corresponds to the center of the dummy head. The distances between the microphones at an azimuth angle of 90° in the horizontal plane and the ipsilateral ear were set to 20, 30, 50, 70, 100, 136, 170 and 200 cm.

The microphones were powered and amplified by a *STUDER LMS Carouso Mic24 ADAT* preamplifier. The measurement signal was played back and simultaneously recorded with a *RME Digiface HDSP Hammerfall* audio card at 48 kHz sampling rate. Impulse responses were measured with logarithmic swept sines [17] with a length of $N = 2^{16}$ samples.

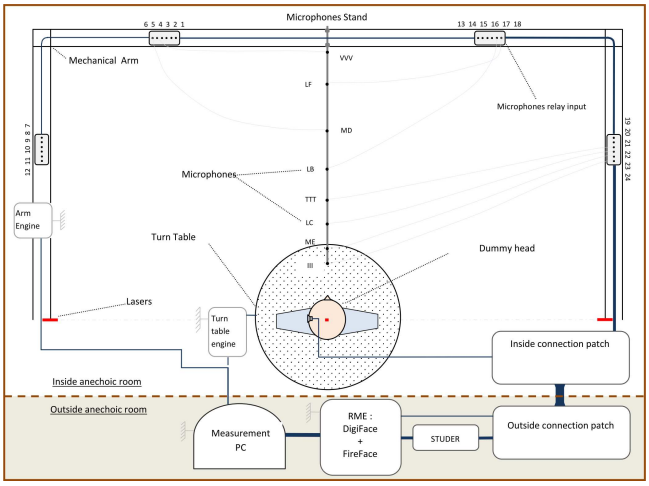

Figure 1: Reverse HRTF measurement of a dummy head at different radial distances.

2.2. Measurement procedure

The measurement procedure was automatically controlled by Matlab® using Max/MSP® as peripheral audio application for data acquisition, and different control sequences to position the rotating arm and the turntable.

First, the dummy head was positioned at azimuth and elevation 0° using the 2 horizontal laser beams for aligning the interaural axis with the measurement device. Then, the elevation of the rotating arm was set to -30°; before starting the measurements an idle time was set to avoid vibrations of the mechanical arm. The measurement signal was emitted from the in-ear loudspeaker and recorded by the microphone array. Next, the turntable was step-wise moved to the next azimuth angle. At the end of a full turn-around the elevation angle is set to a new value and the procedure continues until 90° elevation are reached. A set of N_{points} = 865 impulse responses was measured for each microphone, providing sampling points from -30° to 90° elevation and 360° azimuth, with a step size of 10° in elevation and 5° in azimuth.

2.3. Equalization and preprocessing

All microphones have been equalized to compensate for temporal, phase and level differences. To account for the propagation delays of different measurement positions the time-lag of the closest microphone at ipsilateral position was defined as global temporal reference point. The measurement time frame was set to 2048 samples, with the onset of the reference head related impulse response (HRIR) at 100 samples. Therefore, the relative delay for each microphone and measurement position was within this time frame.

Diffuse-field equalization filters, as described in [18, 19], have been applied to all measurements. These filters are derived from a weighted average over all measurements for one microphone at a known distance; the applied weighting coefficients correspond to the Voronoi surfaces [20] associated with each measurement position. After the diffuse field equalization, directional transfer functions (DTFs) are obtained; one should note that they do not contain distance information anymore. However, range extrapolation methods require to preserve distance attenuation characteristics. As a consequence, a correction gain was applied to the DTFs. The microphone closest to the head is considered as the reference level. The maximum energy of the diffuse field for this reference microphone is computed. The correction gain is defined as the ratio of maximum diffuse-field energy of each microphone and the reference microphone.

3. INTERPOLATION AND RANGE EXTRAPOLATION APPLYING SPHERICAL ACOUSTICS

3.1. Spherical harmonics method

The following section summarizes the theory of spherical interpolation and range extrapolation methods for HRTFs and the reciprocity measurement method used within this article. It mainly follows the theoretical considerations as presented in [13].

The solution of the wave equation in spherical coordinates, under the assumption of negligible incoming waves, yields the following expansion for the acoustic pressure field p with

wavenumber $k = 2\pi f/c$ at the point (r, θ, ϕ) in space

$$p(r, \theta, \phi, k) = \sum_{n=0}^{+\infty} \sum_{m=-n}^{n} a_{nm}(r, k) Y_n^m(\theta, \phi) \quad (1)$$

Y_n^m denotes the complex spherical harmonic function of degree n and order m

$$Y_n^m(\theta, \phi) = (-1)^m \sqrt{\frac{2n+1}{4\pi} \frac{(n-|m|)!}{(n+|m|)!}} P_n^{|m|}(cos\theta) e^{im\phi} \quad (2)$$

and

$$a_{nm}(r, k) = b_{nm}(k) h_n(kr) \quad (3)$$

where h_n denotes the spherical Hankel functions of the first kind associated to the outgoing component of the sound field, and $P_n^{|m|}$ the associated Legendre polynomials. $b_{nm}(k)$ are the spherical expansion coefficients, which have to be determined by a projection-based analysis. The functions Y_n^m and a_{nm} describe the angular and the radial dependency of the sound field, respectively.

Considering two concentric measurement spheres, one can note from (1) that for a given wavenumber k the full-space pressure field is entirely determined by the spherical harmonics expansion coefficients $b_{nm}(k)$. The prediction of HRTFs is thus realized in two processing steps: (a) the measured sound field is expanded into spherical harmonics on a measurement sphere with radius r_0 determining the expansion coefficients $a_{nm}(r_0, k)$ and $b_{nm}(k)$, and (b) the sound field at a target radius r_1 is calculated by applying the spherical Hankel functions as

$$b_{nm}(k) = \frac{a_{nm}(r_0, k)}{h_n(kr_0)} = \frac{a_{nm}(r_1, k)}{h_n(kr_1)} \quad (4)$$

In practice, the outer summation in (1) is truncated at orders $n \leq N$, which corresponds to a spatial band limitation. Rewriting (1) in vector/matrix-notation yields the following system of linear equations

$$\mathbf{p}(r_0, k) = \mathbf{Y}\mathbf{a}(r_0, k) \quad (5)$$

where $\mathbf{p}(r_0, k)$ denotes the N_{points} sound pressure vector, $\mathbf{Y}$ the $N_{points} \times (N+1)^2$ matrix of spherical harmonics up to the order $(N+1)^2 \leq N_{points}$, and $\mathbf{a}(r_0, k)$ the $(N+1)^2$ vector of expansion coefficients.

The spherical harmonics decomposition, *i.e.* solving (5) for the spherical harmonics coefficients $\mathbf{a}(r_0, k)$, requires the inversion of matrix $\mathbf{Y}$. Depending on the distribution of measurement points on the sphere this inversion problem can be ill-posed. In [12] the most appropriate solving method for different sampling grids (Gaussian, irregularly sampled, open or closed grids) was determined. In this study, the measurement grid is a non Gaussian open grid with no data captured below -30° elevation, which is also referred to as the polar gap problem in literature. A least-squares method with Tikhonov regularization was applied to obtain the pseudoinverse of $\mathbf{Y}$

$$pinv(\mathbf{Y}) = (\mathbf{Y}^H \mathbf{W} \mathbf{Y} + \epsilon \mathbf{R})^{-1} \mathbf{W} \mathbf{Y}^H \quad (6)$$

where $\mathbf{W}$ is a diagonal matrix of weighting coefficients to guarantee the orthonormality of the spherical harmonic basis. The weights are obtained by the Voronoi surfaces associated with each measurement point.

With reference to [13], the regularization coefficient ϵ was set to $\epsilon = 10^{-6}$, and the diagonal regularization matrix to $\mathbf{R} = (1 + n(n+1))\mathbf{I}$, where $\mathbf{I}$ denotes the identity matrix and n the degree of the spherical harmonics. As mentioned in [12] the Matlab Regularization Toolbox [21] offers various tools for the analysis and regularization of ill-posed problems, and further allows to automatically determine the regularization parameters. Given the $N_{points} = 865$ spatial sampling points for each measurement distance from the head the order of decomposition was set to $N = 28$; one should note that without regularization the inversion problem is ill-posed and numerically unstable for orders $N > 13$.

The measured data at a known distance allows for evaluating the HRTFs at any angular position by means of the spherical harmonics expansion with the coefficients $a(r_0, k)$ given in (6); the reproduction accuracy is limited by the order truncation, hence the spatial band limitations and aliasing artifacts. The range extrapolation problem can be solved by applying the radial functions to compute the spherical harmonic coefficients $\mathbf{a}(r_1, k)$ at distance r_1

$$\mathbf{a}(r_1, k) = \mathbf{a}(r_0, k) \frac{h_n(kr_1)}{h_n(kr_0)} \quad (7)$$

and applying them to (1). To avoid artifacts due to the exponential growth of the spherical Hankel function of higher-degrees and for small arguments kr the truncation number is limited to $N = kr_{min}$, where r_{min} is the minimum radius of the sphere enclosing the listener's head, *i.e.* the radiating source [10, 13].

3.2. Direct reconstruction and radial propagation

The present study aims to evaluate the accuracy of HRTF range extrapolation in the proximity of a listener's head. For this purpose, measurement data was captured on eight (partial) spheres with different radii around a dummy head, cf. Sec. 2. On each measurement sphere, the HRTFs are expanded into spherical harmonics up to a given order, as has been discussed in Sec. 3.1. The angular interpolation is given in (5) and the range extrapolation with frequency-dependent order truncation in (7).

The following section discusses the simulation results and compares the spherical harmonics method to other near-field HRTF range extrapolation methods proposed in literature. All simulation results for angular interpolation and range extrapolation from near-field to far-field and vice versa are compared against measurement data.

4. ANALYSIS OF SIMULATION RESULTS: PREDICTION ERROR BETWEEN MEASURED AND RECONSTRUCTED HRTFS

In this section the accuracy of the abovementioned angular interpolation and range extrapolation algorithms is determined by comparing measured and synthesized HRTFs. The truncation order for simulations was set to $N = 28$ and regularization was applied, cf. Sec. 3.1. One should note that, due to the poor low frequency response of the emitting in-ear loudspeaker, the comparisons are limited to a frequency range of 1 kHz – 16 kHz. Fig. 2 shows the measured and reconstructed magnitude spectrum of HRTFs in the horizontal plane at a distance of 30 cm and 200 cm from the head.

In the following sections the reconstruction error of the spherical acoustics method is examined. This requires the introduction of a spectral distortion measure to quantify the similarity

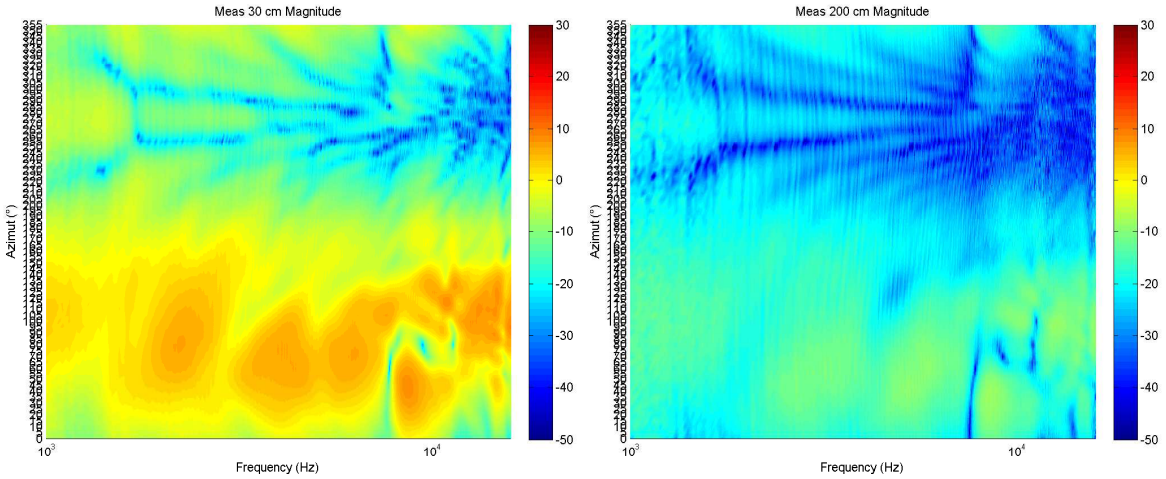

(a) Measured HRTFs at 30 cm

(b) Measured HRTFs at 200 cm

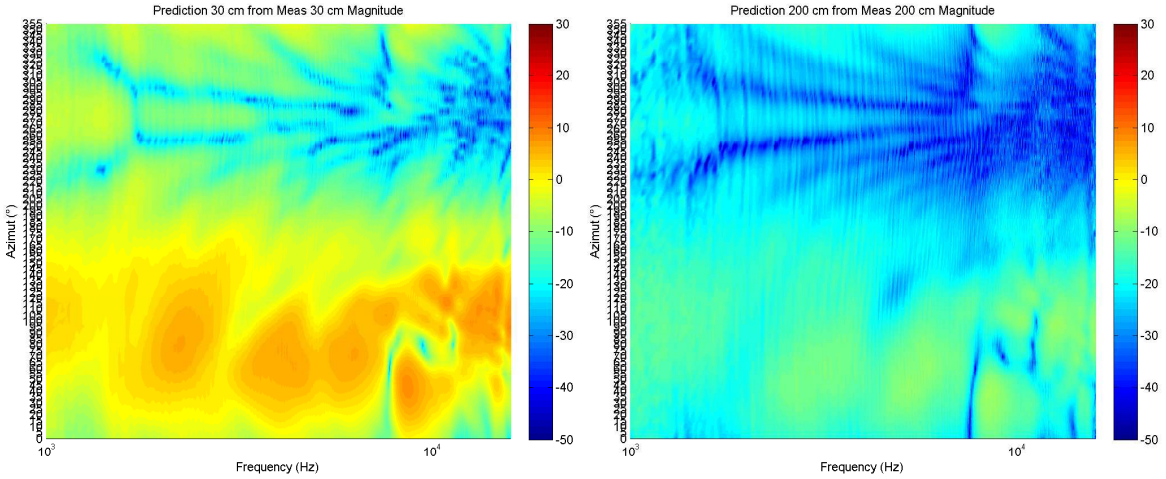

(c) Spherical harmonics expansion of HRTFs at 30 cm

(d) Spherical harmonics expansion of HRTFs at 200 cm

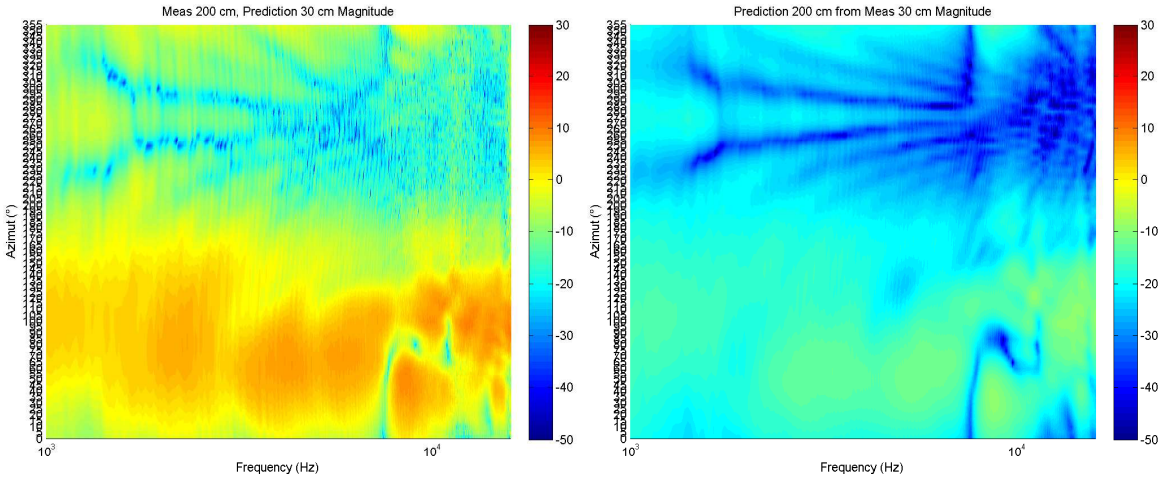

(e) Spherical harmonics expansion of HRTFs at 200 cm and range extrapolation to 30 cm

(f) Spherical harmonics expansion of HRTFs at 30 cm and range extrapolation to 200 cm

Figure 2: Comparison of measured and synthesized HRTFs at 30 cm and 200 cm distance from the head.

between predicted, H_{pred}, and measured, H_{meas}, HRTFs.

$$e(\omega_i) = \frac{1}{N_{points}} \sum_{\ell=1}^{N_{points}} \frac{|H_{pred}(\omega_i, \ell)| - |H_{meas}(\omega_i, \ell)|}{|H_{meas}(\omega_i, \ell)|} \tag{8}$$

This error measure is applied to each spatial sampling point and further averaged for each frequency bin, $\omega_i = 2\pi f_i$, over the entire sphere. Additional spectral smoothing is performed by applying frequency-dependent semitone smoothing windows to the spatially averaged magnitude spectrum. To obtain a single-value error measure the smoothed spectrum is further averaged over frequency. Simulation results have shown a considerable increase of spectral distortions for frequencies above 7 kHz. To adjust the error measure to this frequency-dependent behavior, averaging is performed over two different frequency bands, from 1 kHz to 7 kHz and from 7 kHz to 16 kHz.

4.1. Angular reconstruction

A good agreement of measured and reconstructed HRTFs on a sphere of given radius can be observed by comparing Figs. 2(a) to 2(d). The average reconstruction error is shown in Fig. 3; to illustrate its dependence on the signal-to-noise ratio, the SNR is given for each measurement distance. The average reconstruction error ranges from -80 dB to -30 dB and increases with the measurement distance.

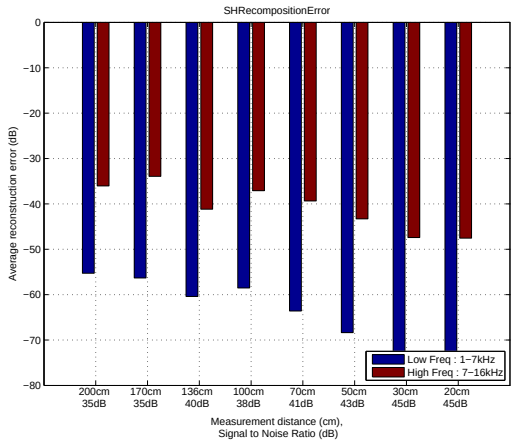

Figure 3: Spectral distortion of spherical harmonics HRTF resynthesis at 8 different measurement distances from the head. The second value indicates the SNR at each measurement point.

4.2. Range extrapolation

Fig. 2 illustrates that range extrapolation deteriorates HRTF reconstruction, *e.g.* extrapolation from far-field to near-field results in an irregular and fuzzy magnitude spectrum for contralateral HRTFs. In the following sections the simulation results are discussed in more detail.

4.2.1. HRTF reconstruction at different target distances from a measurement distance:

The average spectral reconstruction error of the spherical acoustics method for different target distances, derived from a known measurement distance, is illustrated in Fig. 4. The reconstruction error is shown for range extrapolation to the far-field (4(a)) and to the near-field (4(b)), respectively. Results are presented for measurements at distances 30 cm and 200 cm from the head.

Different target distances: Fig. 4 clearly shows higher errors at 70 and 100 cm from the head than for all other distances. The same trend could be observed for HRTFs derived from other measurement distances. This is probably due to the fact that the measurement microphones have not been matched in sensitivity and frequency differences, even though their frequency responses were carefully equalized before applying spherical harmonics transform.

Near-field to far-field vs. far-field to near-field prediction: In Fig. 2 one can easily see that far-field prediction of HRTFs is more accurate than near-field prediction, especially at high frequencies. Figs. 4(a) and 4(b) further illustrate this behavior showing (a) no significant differences of the error measure at lower frequencies and (b) increasing reproduction errors with distance for higher-frequencies, especially for range extrapolation to the far-field.

4.2.2. HRTF reconstruction at a target distance from different measurement distances

The reconstruction error for a target distance as a function of the measurement distances is illustrated in Fig. 5. Again, it can be shown that at low frequencies far-field and near-field prediction errors are very similar. The near field prediction error in Fig. 5(a) increases with increasing measurement distance at high frequencies. The far-field prediction error, as shown in Fig. 5(b), is independent of the frequency and measurement distance.

5. COMPARISON OF RANGE EXTRAPOLATION APPLYING SPHERICAL ACOUSTICS WITH OTHER DISTANCE COMPENSATION METHODS

This section compares spherical acoustic range extrapolation of HRTFs with other methods proposed in literature, such as the inverse distance attenuation coefficient, near-field compensation filters [15], and the selection of HRTFs [8]. All range extrapolation methods have been applied to a basis of HRTFs at radius r_0; angular interpolation of HRTFs was done by spherical harmonics expansion, which has been found as sufficiently accurate in Sec. 4.1.

The first method, which is further referred to as *distance attenuation method*, applies a simple distance attenuation factor $g(r_i) = r_i/r_0$. The second radial extrapolation method, referred to as *compensation filter method*, applies distance compensation filters [8] derived from a spherical head model evaluated at distances r_1 and r_0 [15]. The third method, in the following referred to as *cross-ear selection method*, further extends the near-field compensation filter method by monaural gain corrections and a geometrically derived selection of HRTFs depending on the relative position of the source to the respective ear.

The reconstructed HRTFs are compared to measurement data applying the error measure derived in Sec. 4. To ease comparisons with the cross-ear selection method, error measure calculations are restricted to the horizontal plane. The comparison results are summarized in Fig. 6.

For far-field to near-field prediction and low frequencies the spherical acoustics method shows the lowest reconstruction error of all methods, Fig. 6(a); its reconstruction error is 10 dB less

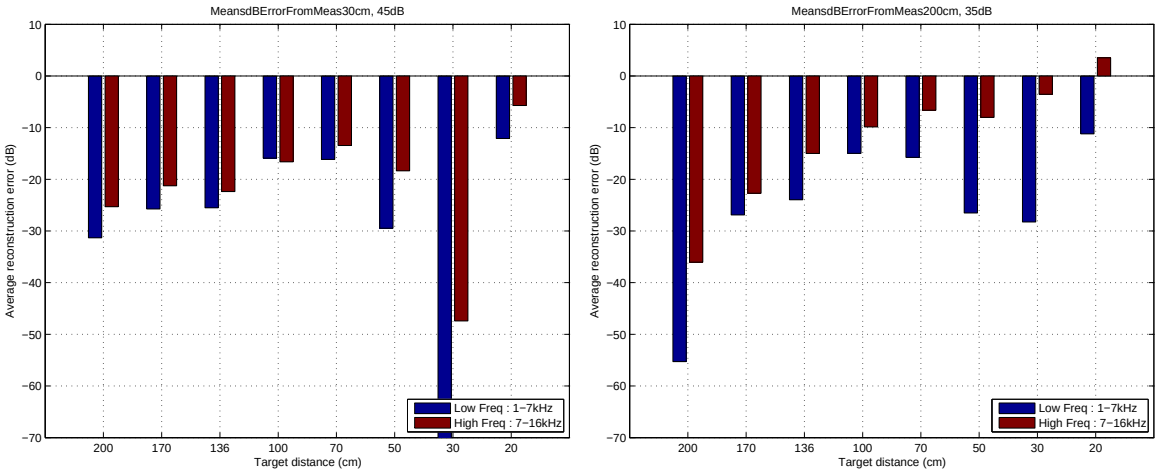

(a) Far-field prediction from measurements at 30 cm (b) Near-field prediction from measurements at 200 cm

Figure 4: Average spectral reconstruction error of the spherical acoustics method: HRTFs reconstructed at 8 different target distances from measurements at (a) 30 cm, thus mostly (except for target at 20 cm) representing range extrapolation to the far-field, and (b) 200 cm, thus representing range extrapolation to the near-field.

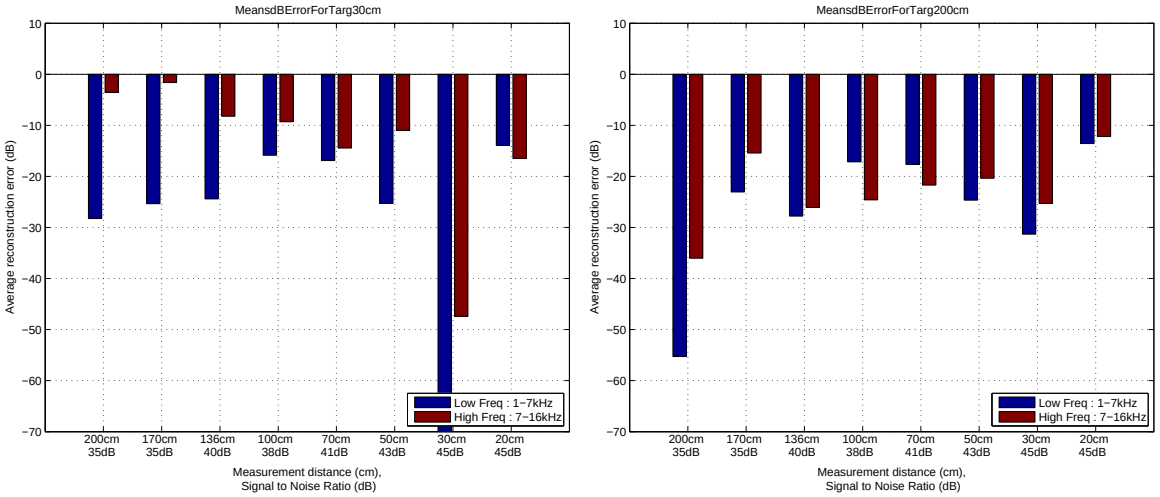

(a) Near-field prediction of a target at 30 cm (b) Far-field prediction of a target at 200 cm

Figure 5: Average spectral reconstruction error of the spherical acoustics method: HRTFs reconstructed at (a) 30 cm and (b) 200 cm from measurements at 8 different distances, thus mostly representing near-field and far-field prediction, respectively. The second value indicates the SNR at each measurement point.

than *e.g.* for the distance attenuation method. One can further observe that a higher complexity of rendering results in lower reconstruction errors. The reconstruction error decreases from simple distance attenuation to the crossear selection method. Even though the spherical harmonics method performs best for near-field prediction at low frequencies it does poorly at high frequencies; it is even outperformed by simple and computationally efficient distance attenuation.

For near-field to far-field prediction, Fig. 6(b), the different methods performed very similar. The reconstruction error of the spherical acoustics method was slightly better than for the other methods, the crossear selection method was less accurate.

6. DISCUSSION

6.1. Angular interpolation

The spherical harmonics expansion for angular interpolation of HRTFs shows similar results to the ones reported in [5, 12]. In addition, the open measurement sphere yields ill-conditioning and rendering artifacts, which can be minimized by applying different regularization methods. The HRTF reproduction accuracy also depends on the radius of the measurement sphere, *i.e.* the measurement SNR decreases with distance from the head and the spatial sampling grid becomes sparser. As a consequence, it is difficult to correctly determine high spatial variations of a ra-

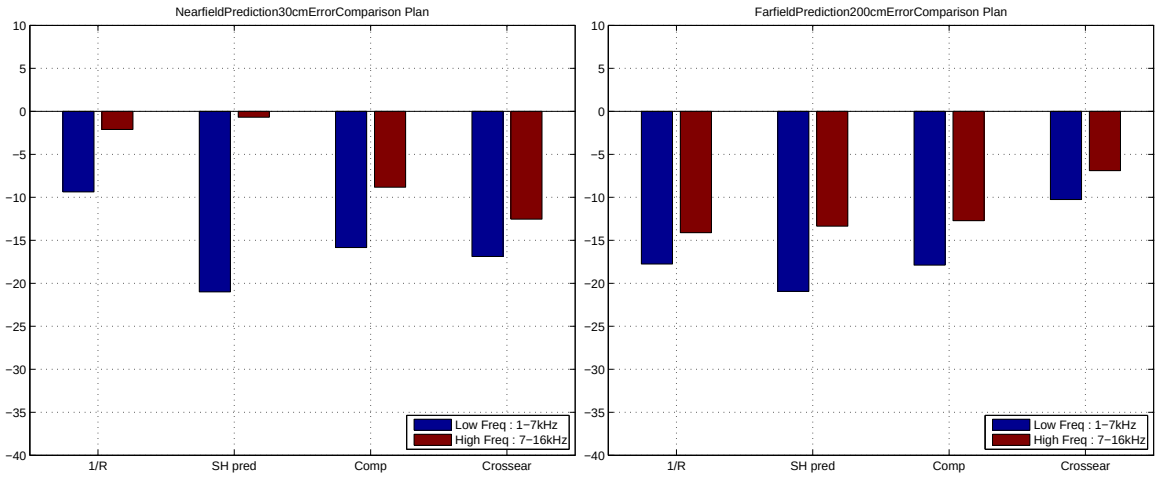

(a) Near-field prediction at 30 cm (b) Far-field prediction at 200 cm

Figure 6: Comparison of range extrapolation with spherical acoustics and other distance attenuation methods for (a) far-field to near-field (from 200 cm to 30 cm) and (b) near-field to far-field (from 30 cm to 200 cm) HRTF prediction.

diating source near the origin from measurements far away [10].

6.2. Range extrapolation

The agreement between measured and reconstructed HRTFs for range extrapolation is not as exact as for angular interpolation; this corresponds to the observations published in [13]. In the case of far-field to near-field prediction strong and audible artifacts occure at high frequencies, especially for contralateral HRTFs in the proximity of the head. The average spectral error measure, introduced in Sec. 4, clearly shows that near-field prediction becomes inaccurate at high frequencies whereas the far-field prediction error remains nearby constant for low and high frequency bands.

The differences between near-field and far-field prediction mainly result from the very low SNR and the sparse spatial sampling grid of far-field measurements. Noise can cause divergences at small radii, *i.e.* when the argument kr becomes smaller than N, due to the exponential growth of the spherical Hankel functions towards the center of the measurement sphere. The sparse spatial sampling at far-field distances previously discussed further biases the results [10].

Even though all microphones have been equalized before measurements, the simulation results reveal an increase of the measurement error for three microphone distances, cf. Sec. 4.2. This behavior could not be explained from theory, so the data has to be further analyzed to determine the cause of this systematic measurement error.

Accurate synthesis of HRTFs by spherical harmonics expansion of measurement data on a single sphere is possible. It can be shown that the range extrapolation from near-field to far-field clearly outperforms the far-field to near-field prediction. For this reason one would rather measure a full set of HRTFs in the near-field of the head and extrapolate the data to the far-field than vice versa.

6.3. Comparisons with other range extrapolation methods

The spherical acoustics method for range extrapolation of HRTFs does not generally perform better than other methods proposed in literature, cf. Sec. 4.2. In the frequency range up to 7 kHz it could be proven as being more accurate for both the near-field and far-field prediction of HRTFs; the agreement between measured and predicted data is good. For range extrapolation from the near-field to the far-field and frequencies above 7 kHz all methods resulted in comparable averaged spectral distortions errors. However, for the extrapolation from the far-field to the near-field and frequencies above 7 kHz the spherical acoustics method yielded strong spectral distortions, which strongly depend on the measurement SNR. Due to the limited acoustic power of the emitting in-ear loudspeaker, the reciprocity method results in a low SNR. A hybrid approach for near-field prediction, combining the spherical acoustics method for low frequencies and crossear selection method for high frequencies, could be used for accurate synthesis of HRTFs from given far-field measurements.

Binaural rendering systems mostly often apply computationally efficient models of HRTFs, such as biquad filters – distance attenuation, near-field compensation, and cross-ear selection can be directly applied to these filter models. The spherical acoustics method implies decoding the spherical harmonic coefficients and applying the radial propagation terms to obtain the transfer function for a desired position on space. The choice is then either to directly convolve the signals with this HRTF (or the corresponding impulse response) or to derive a computationally more efficient filter. In terms of real-time computing, range extrapolation with spherical acoustics requires more computational power than other distance rendering methods. For an optimal use of the spherical acoustic method for distance prediction, a solution could be derived from [9]. It consists in pre-computing a database of near-field HRTFs at different distances and only switch in between HRTFs when it is perceptually necessary.

7. CONCLUSION

This paper has been concerned with the prediction of head related transfer functions (HRTFs) in the proximity of the head from measurements at a given distance using spherical acoustics. The accuracy of angular interpolation and range extrapolation was determined by comparing measured and synthesized HRTFs at different distances from the head.

The agreement between measured and predicted data was good, but it could be shown that the range extrapolation from near-field to far-field clearly outperforms the far-field to near-field prediction of HRTFs. A variety of other range extrapolation comprising inverse distance attenuation, near-Þeld compensation filters, and the selection of HRTFs have been compared against the proposed method, which was proven as to be more accurate except for high frequencies and near-field prediction.

In the future, subjective listening experiments with individually measured HRTFs should be carried out to investigate the perceptual impact of the artifacts caused by the different prediction methods.

8. REFERENCES

[1] E. H. A. Langendijk and A. W. Bronkhorst, "Fidelity of three-dimensional-sound reproduction using a virtual auditory display," *J. Acoust. Soc. Am.*, vol. 107, no. 1, pp. 528–537, 2000.

[2] V. Larcher and J. M. Jot, "Techniques d'interpolation de filtres audio-numériques, Application à la reproduction spatiale des sons sur écouteurs." in *Congres Français d'Acoustique (CFA), Marseille, France*, 1997.

[3] D. J. Kistler and F. L. Wightman, "A model of head-related transfer functions based on principal components analysis and minimum-phase reconstruction." *J. Acoust. Soc. Am.*, vol. 91, no. 3, pp. 1637–1647, 1992.

[4] J. Chen, B. D. Van Veen, and K. E. Hecox, "A spatial feature extraction and regularization model for the head-related transfer function a)," *J. Acoust. Soc. Am*, vol. 97, no. 1, pp. 439–452, 1995.

[5] M. J. Evans, J. A. S. Angus, and A. I. Tew, "Analyzing head-related transfer function measurements using surface spherical harmonics," *J. Acoust. Soc. Am.*, vol. 104, no. 4, pp. 2400–2411, 1998.

[6] D. S. Brungart and W. M. Rabinowitz, "Auditory localization of nearby sources. Head-related transfer functions," *J. Acoust. Soc. Am.*, vol. 106, no. 3, pp. 1465–1479, 1999.

[7] P. Zahorik, D. S. Brungart, and A. W. Bronkhorst, "Auditory distance perception in humans: A summary of past and present research," *Acta Acustica united with Acustica*, vol. 91, no. 3, pp. 409–420, 2005.

[8] D. Romblom and B. Cook, "Near-field compensation for HRTF processing," in *125th Conv. Audio Eng. Soc., San Francisco, CA, USA*, no. 7611, 2008.

[9] T. Lentz, I. Assenmacher, M. Vorländer, and T. Kuhlen, "Precise Near-to-Head Acoustics with Binaural Synthesis," *Journal of Virtual Reality and Broadcasting*, vol. 3, no. 2, 2006.

[10] G. Weinreich and E. B. Arnold, "Method for measuring acoustic radiation fields," *J. Acoust. Soc. Am.*, vol. 68, no. 2, pp. 404–411, 1980.

[11] E. G. Williams, *Fourier Acoustics: Sound Radiation and Nearfield Acoustical Holography*. Academic Pr, 1999.

[12] D. N. Zotkin, R. Duraiswami, and N. A. Gumerov, "Regularized HRTF fitting using spherical harmonics," in *IEEE WASPAA 2009, New Paltz, NY, USA*, 2009.

[13] R. Duraiswami, D. N. Zotkin, and N. A. Gumerov, "Interpolation and range extrapolation of HRTFs," in *IEEE ICASSP 2004, Montreal, QC, Canada*, 2004, pp. 45–48.

[14] W. Zhang, T. D. Abhayapala, R. A. Kennedy, and R. Duraiswami, "Modal expansion of HRTFs: Continuous representation in frequency-range-angle," in *ICASSP, Los Alamitos, CA, USA*. IEEE Computer Society, 2009, pp. 285–288.

[15] R. O. Duda and W. L. Martens, "Range dependence of the response of a spherical head model," *J. Acoust. Soc. Am.*, vol. 104, no. 5, pp. 3048–3058, 1998.

[16] D. N. Zotkin, R. Duraiswami, E. Grassi, and N. A. Gumerov, "Fast head-related transfer function measurement via reciprocity," *J. Acoust. Soc. Am.*, vol. 120, no. 4, pp. 2202–2215, 2006.

[17] A. Farina, "Simultaneous measurement of impulse response and distortion with a swept-sine technique," in *110th Conv. Audio Eng. Soc., Paris, France*, no. 5093, 2000.

[18] V. Larcher, G. Vandernoot, and J. M. Jot, "Equalization methods in binaural technology," in *105th Conv. Audio Eng. Soc., San Francisco, CA, USA*, no. 4858, 1998, pp. 26–29.

[19] V. Larcher, "Techniques de spatialisation des sons pour la réalité virtuelle," Ph.D. dissertation, Université Paris VI, 2001.

[20] H. S. Na, C. N. Lee, and O. Cheong, "Voronoi diagrams on the sphere," *Computational Geometry*, vol. 23, no. 2, pp. 183–194, 2002.

[21] P. C. Hansen, "Regularization tools: A Matlab package for analysis and solution of discrete ill-posed problems," *Numerical Algorithms*, vol. 6, no. 1, pp. 1–35, 1994.